



Revista Facultad de Ingeniería  
Universidad de Antioquia

ISSN: 0120-6230

revistaingenieria@udea.edu.co

Universidad de Antioquia  
Colombia

Kannabiran, Kanimozhi; Alagarsamy, Shunmugalatha  
Unified control of DC-DC buck converter using dynamic adaptive controller for battery  
operated devices  
Revista Facultad de Ingeniería Universidad de Antioquia, núm. 81, diciembre, 2016, pp.  
35-46  
Universidad de Antioquia  
Medellín, Colombia

Available in: <http://www.redalyc.org/articulo.oa?id=43048640003>

- How to cite
- Complete issue
- More information about this article
- Journal's homepage in redalyc.org

redalyc.org

Scientific Information System

Network of Scientific Journals from Latin America, the Caribbean, Spain and Portugal

Non-profit academic project, developed under the open access initiative

# Unified control of DC-DC buck converter using dynamic adaptive controller for battery operated devices



Control unificado de convertidor buck DC- DC utilizando controlador adaptativo dinámico para dispositivos que funcionan con baterías

Kanimozhi Kannabiran<sup>1</sup>, Shunmugalatha Alagarsamy<sup>2</sup>

<sup>1</sup>Department of Electrical and Electronics Engineering, ULTRA College of Engineering and Technology for Women. Ultra Nagar, Madurai-Chennai Highway, Madurai - 625 104. Madurai, India.

<sup>2</sup>Department of Electrical and Electronics Engineering, Velammal College of Engineering and Technology. Madurai to Rameshwaram High Road, Viraganoor, Madurai-625009. Madurai, India.

## ARTICLE INFO

Received February 15, 2015

Accepted July 15, 2016

## KEYWORDS

Pulse width modulation, adaptive sliding mode control, buck converter, gain scheduling, Lyapunov stability

Modulación de ancho, control por modos deslizantes adaptativos, convertidor buck, ganancia programación, estabilidad de Lyapunov

**ABSTRACT:** The objective of this paper is improving the dynamic response of DC-DC converter system with internal parameter uncertainties. The methodology of sliding mode control in existing works is based on Proportional Integral and Derivative Controller (PID). The present work addresses various issues on a unified approach for design and application of pulse-width modulation (PWM) based on Digital Adaptive Sliding Mode equivalent (ASM) control technique to buck converter for mobile phones operating in continuous conduction mode (CCM), and discontinuous conduction mode (DCM). The controller is gain scheduled to monitor the output loading condition, and adaptively changes the control parameters to give an optimum dynamic performance corresponding to any load variations. Further stability is analytically verified using Lyapunov stability criterion and the system is proved to be globally asymptotically stable. Finally, the effectiveness of the proposed method is verified by simulation and experiment. Stable steady state response with reduced ripple is obtained.

**RESUMEN:** El objetivo de esta investigación es mejorar la respuesta dinámica del sistema de convertidor DC-DC con incertidumbres en los parámetros internos. La metodología de control por modo deslizante en las obras existentes se basa en un sistema de control proporcional-integral-derivativo (PID). El presente trabajo aborda diversas cuestiones en un enfoque unificado para el diseño y la aplicación de la modulación de ancho de pulso (PWM) basado en control digital por modos deslizantes adaptativos (CMD), técnica de control para el controlador buck para los teléfonos móviles que funcionan en modo continuo de conducción (MCC) y el modo de conducción discontinua (MCD). El controlador está programado para controlar la ganancia de la condición de carga de salida y cambiar adaptativamente los parámetros de control para dar un rendimiento dinámico óptimo correspondiente a las variaciones de carga. Además, la estabilidad se verifica analíticamente utilizando el criterio de estabilidad de Lyapunov y se prueba que el sistema es global y asintóticamente estable. Finalmente, la eficacia del método propuesto se verifica mediante la simulación y experimentación. Se obtiene una respuesta estable en estado estacionario con ondulación reducida.

## 1. Introduction

In power converters, a high premium is placed on the efficiency of power conversion, besides steady state and dynamic performance. The switching property makes the power converters prime candidates for the application of

the theory of Variable Structure Systems (VSSs). VSS theory results in a time domain description of switching converters. Switched mode DC-DC converters are nonlinear and time invariant systems. The difficulty in control of output voltage is owing to non - minimal phase nature of these converters, since the control inputs appear both in voltage and current equations. This typically makes the transient response of the system sluggish. The analysis and design of a hysteretic PWM controller with improved transient response have been proposed for buck converter and Voltage-mode hysteretic controllers for synchronous buck converter used for many automobile applications [1].

\* Corresponding author: Kanimozhi Kannabiran  
e-mail: kanilalith2003@gmail.com  
ISSN 0120-6230  
e-ISSN 2422-2844



Nonlinear control schemes, such as one-cycle control, current-mode control and sliding-mode control (SMC), have been discussed for DC-DC converters [2]. Among them, SMC has advantages such as simple implementation, insensitive to parameter changes. The Sliding Mode controller (SMC) is a nonlinear controller introduced for controlling (VSSs) [3].

Adaptive hysteresis control is applied for fixing the switching frequency of SMC. But non-Zero steady-state error cannot be achieved. In spite of achieving constant switching frequency with a sliding surface equivalent control only with the output voltage sensed [4], there are low frequency oscillations on the output waveform. The controller is based on an exact model without considering power losses. Power losses can also be considered in designing SMC for converters [5].

Predictive SM controlled converter has faster dynamic response with reduced steady state error when it is operated above the nominal load, and it eliminates overshoots and ringing in the transient response when operated below the nominal load [6]. An adaptive feed forward control that varies the hysteresis band in the hysteresis modulator of the SM controller in the event of any change of the line input voltage and for load variation, and adaptive feedback controller that varies the control parameters with the change of output load is proposed by Tan [7]. The advantages of good transient response and robustness to uncertainties are indicated in comparison with a conventional proportional-integral control system [8] and a conventional SMC scheme [9].

The detailed discussion of SM control theory and the relationship of SM control and duty ratio control, can be found in [10, 11]. The ineffectiveness of conventional SM controlled converters is inferred from the degradation of dynamic and steady state performance for load variations [12]. Investigations on overshoots and ringing during a transient state under nominal load and when operated above the nominal load discussed in [13] concluded that the response will be slow with a high steady state error.

Second-order SM control algorithm has been applied to buck converter for reduction of chattering [14]. Two types of SM-control for boost and buck-boost converters: one using the method of stable system center [15] and the other using sliding dynamic manifold are discussed [16]. A nonlinear control technique called Adaptive Sliding Mode (ASM) control technique working at DCM has been discussed [17]. The controller is based on the exact model without considering power losses. However, this controller slows down the system response.

The various approaches regarding gain-scheduling are the classical gain-scheduling approach, more recently Linear Parameter varying (LPV) method [18] and thirdly, fuzzy techniques.

A gain-scheduled controller, thus can adjust it self according to the changes in the dynamics of the plant [19]. Recent LPV

control synthesis techniques elaborate on this idea using i) parameter-varying Lyapunov functions and ii) scaled small-gain theorems. A LPV model comprises linear, parameter-dependent dynamics [20].

Low voltage circuits are essential to satisfy the demands of single battery operation in portable electronic devices like cellular phones, pagers, laptop computers, portable device applications, etc. Maximization of battery life, high power efficient DC-DC converters are desirable factors of battery powered devices. Here, load conditions change from high to low power levels i.e. from DCM to CCM. The load does not remain in DCM (heavy load) for long periods, rather these devices operate in CCM (light load) i.e. standby mode most of the time. Therefore, improving light-load efficiency of DC-DC converters are crucial for extending battery life.

This paper aims to improve previous controller [21] by modeling system with power losses to improve system performance. A gain scheduled Digital, ASM equivalent voltage mode controller working at CCM and DCM that optimizes the dynamic performance during a wide range of load variations for mobile phones is proposed. The converter is modeled with power losses and this model is simplified to incorporate the proposed simple adaptive algorithm. Finally, the proposed controller is applied. This is implemented through the incorporation of a gain scheduling scheme into the conventional SM controller. The controller parameters are adaptively varied according to output loading. The work was conducted on a unified topology: buck converter working in both CCM and DCM for mobile phones. This paper aims to present the necessary theoretical background and implementation details that enable the proposed controller to be readily adopted for portable battery applications.

## 2. Proposed approach

Switched networks create non-linear time varying problems. Therefore, switched network modeling has gained importance to improve the response of the system. A modeling procedure for the buck converter case is derived. All the passive elements are assumed to be Linear Time Invariant (LTI) and the switches have only switching loss. The converter is assumed to operate in the CCM and a boundary detector circuit is to be implemented to make it to operate in both modes. A new Equivalent SMC technique to design a controller for mobile batteries is to be used. Design and implementation of a unified ASM controller for buck converter is to be discussed in section 3.

Switching losses in DC-DC converters are due to: MOSFET modeled as a switch on resistor  $r_{sw}$ ; parasitic effect of the inductor modeled as resistor  $r_l$ ; the diode forward voltage drop modeled as a turn on voltage source  $v_d$ . The electrical equivalent circuit for battery operated mobile phone system consists of inductor  $L_E$  and resistor  $R_E$ . A buck converter with the above-mentioned dissipation losses is shown in Figure 1. A model designed considering switching losses improves efficiency of operation.

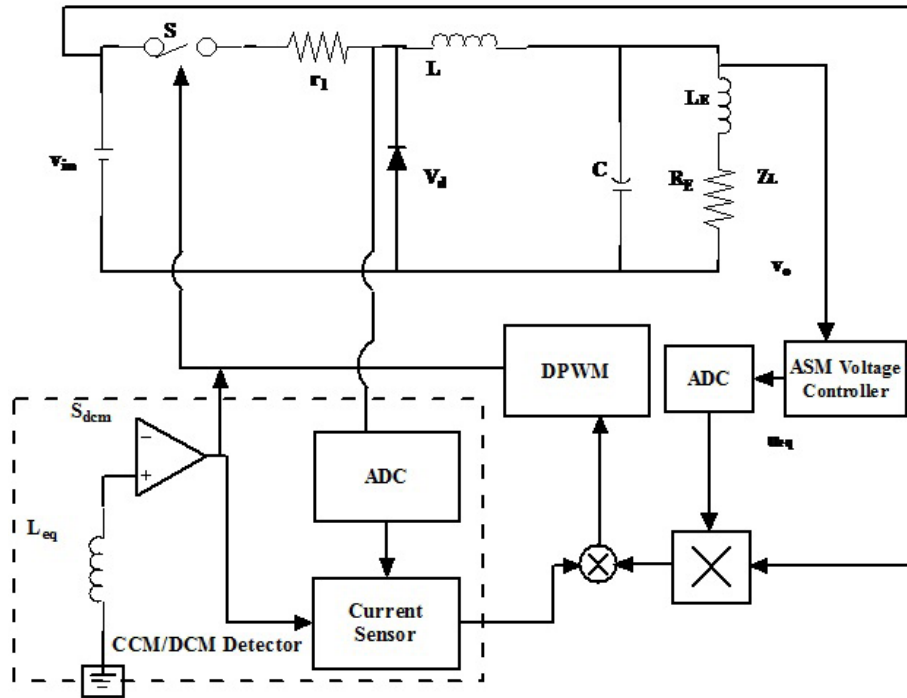


Figure 1 Proposed Block diagram of Buck Converter

## 2.1. Modeling of converter with losses

Design of an SM controller starts with a state-space description of the converter model in terms of the desired control variable, ie. Voltage. The nomenclature followed in controller design is shown in Table 1. The focus of this paper is the application of SM control to converters operating in CCM and DCM. The PWM repeating period is  $T$  and the switching frequency  $f=1/T$ . The duty cycle is represented as a scalar input  $u$ . The instantaneous values of current and voltage are  $I_x$  and  $V_x$  for the component  $X$ . The input voltage, input current, output voltage and output current are denoted by  $V_{in}$ ,  $I_{in}$ ,  $V_o$  and  $I_o$  respectively. The mobile phone in the circuit is modeled as impedance  $Z_L$ .

The state vectors for the converter are [1]:

$$X = \begin{bmatrix} x_1 \\ x_2 \end{bmatrix} = \begin{bmatrix} I_l \\ v_o \end{bmatrix} \quad (1)$$

The state space equation for the buck converter when the switch is in ON and OFF condition during CCM and DCM is combined and the state space averaged model [2] can be derived as  $\dot{X} = A_3 X + B_3$

For buck Converter

$$A_3 = A_1 \bar{u} + A_2 (1 - \bar{u}) = \begin{bmatrix} -\frac{r_{sw} \bar{u} + r_l}{L} & -\frac{1}{L} \\ \frac{1}{C} & -\frac{1}{Z_L C} \end{bmatrix}$$

$$B_3 = B_1 \bar{u} + B_2 (1 - \bar{u}) = \begin{bmatrix} \frac{V_{in} \bar{u} - V_d (1 - \bar{u})}{L} \\ 0 \end{bmatrix} \quad (2)$$

The converter steady state voltage transfer gain  $M$  [3] is

$$M = \frac{V_o}{V_{in}} = \frac{\bar{u} - \frac{V_d}{V_{in}} (1 - \bar{u})}{1 + \frac{r_{sw} \bar{u} + r_l}{Z_L}} \quad (3)$$

Eqs. (3) and (4) prove the impact of practical components on gain term  $M$ .

For the converter

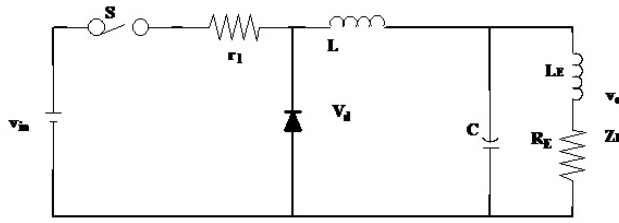
$$A_3 = \begin{bmatrix} -\frac{\bar{u}(r_l + r_{sw})}{L} & \frac{(\bar{u} - 1)}{L} \\ \frac{(1 - \bar{u})}{C} & \frac{\bar{u}}{Z_L C} \end{bmatrix} \quad B_3 = \begin{bmatrix} \frac{V_{in}(1 - \bar{u}) - V_d}{L} \\ 0 \end{bmatrix} \quad (4)$$

The lossy terms at normal operating conditions are  $r_{sw}$ ,  $r_l$

**Table 1 Nomenclature**

Symbol	Description	Symbol	Description
$V_{in}$	Input Voltage	$t_s$	CCM Switching Period
$V_o$	Output Voltage	$\gamma$	Adaptive Coefficient
$d$	Duty Ratio	$i_{ref}$	Reference Current
$i_o$	Output Current	$\overline{u_{eq}}$	Equivalent Control Signal
$k_{sense}$	Feedforward Path Gain	$\overline{u}$	Discontinuous Input Function
$i_c$	Capacitor Current	$x_1, x_2, x_3$	State Variables
$\alpha, \beta$	Sliding Coefficient	$v_r$	Reference Voltage
$i_l$	Inductor Current	$L$	Inductor
$S_{dcm}$	DCM Amplifier Signal	$C$	Capacitor
$t_{dcm}$	Discontinuous Conduction Interval	$L_E$	Load Inductance
$V(x)$	Lyapunov Function	$R_E$	Load Resistance
$t_{osc}$	Dcm Oscillation Period	$Z_L$	Load Impedance

and  $v_d$ . The representation of the practical buck converter is shown in Figure 2.

**Figure 2 Simplified model of Buck Converter**

Steady state voltage transfer gain is shown in [5],

$$M = \frac{(1-\bar{u}) - \frac{V_d}{V_{in}}}{1 + \frac{r_{sw}\bar{u} + r_l}{Z_L}} \quad (5)$$

The final state space averaged equation with single power loss term  $r_{loss}$  is derived as follows [6].

$$\dot{X} = A X + B \bar{u} \quad (6)$$

For the buck converter, the state space averaged model [7], new steady state voltage transfer gain [8], and loss term [9] are shown as follows,

$$A = \begin{bmatrix} -\frac{r_{loss}}{L} & -\frac{1}{L} \\ \frac{1}{C} & -\frac{1}{Z_L C} \end{bmatrix} \quad B = \begin{bmatrix} \frac{V_{in}}{L} \\ 0 \end{bmatrix} \quad (7)$$

$$M_{new} = \frac{v_{out}}{v_{in}} = \frac{Z_L}{Z_L + r_{loss}} \bar{u} \quad (8)$$

$$r_{loss} = \frac{V_{in} \bar{u} (r_l + r_{sw} \bar{u}) + Z_L V_d (1 - \bar{u})}{v_{in} \bar{u} - V_d (1 - \bar{u})} \quad (9)$$

The simplified circuit shown in Figure 2 provides the same response as that obtained from the basic model of converters. Next, the design of a unified controller for buck converter is discussed in section 3.

## 2.2. Adaptive Switching Control for CCM/DCM boundary detections

A Converter operating on the boundary of CCM and DCM is applied at low power levels. This boundary between CCM (heavy load) and DCM (light load) is necessary because the transfer function between duty cycle  $d$  and the output voltage  $v_o$  or between input voltage  $v_{in}$  and output voltage  $v_o$  depends on load condition in DCM. Therefore, to improve the performance, the boundary between CCM and DCM has to be predicted [19]. The aim of the proposed ASMC is to maintain same sliding coefficients for DCM operation. Detection of zero crossings of the inductor current  $i_l$  aids both the high-side and low-side switches to be turned off.

In the CCM/DCM adaptive switching controller proposed in this paper an auxiliary inductor winding and DCM comparator are used to detect zero crossings of inductor current. DCM oscillation period  $t_{osc}$  detected by DCM comparator signal  $S_{dcm}$  is assumed to remain constant between two consecutive periods. On completion of the normal CCM switching period  $t_s$  controller waits for transition of  $S_{dcm}$  from low signal to high signal. Now the MOSFET turn off time is extended by half of  $t_{osc}$ . Therefore,

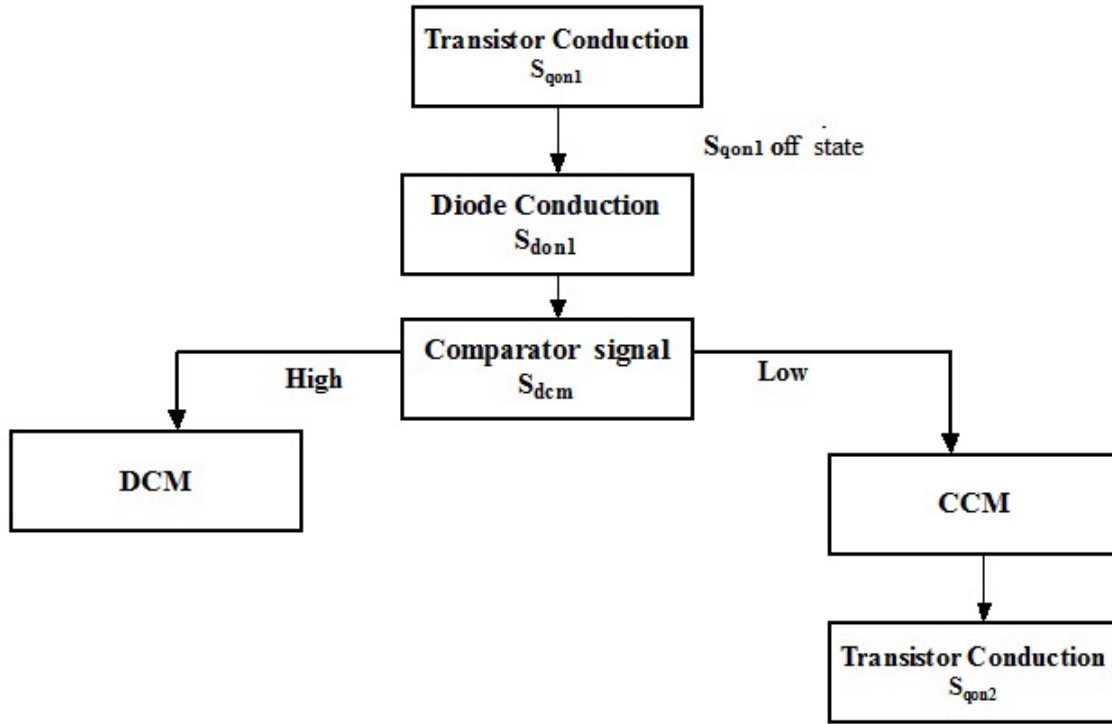


**Figure 3 Control Algorithm for adaptive switching**

the next cycle of DCM ends at a point when  $I$  is zero. This facilitates the calculation of current sensing factor  $k_{sense}$  (10). The discontinuous conduction interval  $t_{dcm}$  is measured and  $k_{sense}$  is calculated as

$$k_{sense} = 1 - \frac{t_{dcm}}{t_s} \quad (10)$$

The illustration of adaptive switching controller is shown in Figure 3.

Using the above algorithm, the adaptive CCM/DCM control law is shown in (11).

$$e_i[n] = t_{sw} \cdot i_{ref} - (t_{sw} - t_{dcm}) i_{lsense} \quad (11)$$

where  $t_{sw}$  is adaptive switching period. From the control chart, we can conclude that the DCM comparator output decides the switching between high level and low level state.

### 3. Proposed digital ASM controller

Buck converters are time variable and a nonlinear switching circuit which possess variable structure features. In the following section, the design of control equations for the proposed method to improve the dynamic response is outlined. A new variation of Sliding mode control of the PWM buck converter is proposed. The detailed procedure for designing unified Digital ASM controller for buck

converters in CCM and DCM operation is discussed in the following section.

#### 3.1. Sliding Mode Control Approach

Design of robust controller is made possible using SMC methodology. The two advantages of this approach are: The dynamic behavior of the system is decided by the particular value of reference chosen for the switching function. Therefore, closed-loop response is not affected by any system uncertainties. The two - step design approach is as follows:

1. Design of a sliding motion switching function to satisfy the design specifications.
2. Selection of a control law to make the switching function feasible for the system state.

Traditional SMC employs a sliding manifold (12) as

$$\sigma(x, t) = SX + \phi = 0 \quad (12)$$

where  $S = [S_1, S_2, S_3, \dots, S_N]$  and  $\phi$  is the reference value obtained from state space equation. If the representing point (RP) slides on the sliding surface  $\sigma(x, t) = 0$  the system is said to be in sliding mode. The existing condition (13) is

$$\lim_{\sigma \rightarrow 0} \sigma \cdot \frac{d\sigma}{dt} < 0 \quad (13)$$

The sufficient condition for the system to reach the sliding surface is if the RP is initially in one subsystem, it will hit

the sliding surface in spite of its initial position in finite time. Considering the system operating over the sliding region, the sliding function satisfies the condition shown in (14).

$$\begin{aligned}\sigma(x,t) &= 0, \frac{d\sigma(x,t)}{dt} = 0 \\ \dot{\sigma}(x,t) &= S\dot{X}\end{aligned}\quad (14)$$

Using Eqs. (7, 12, 13) we get the reaching condition for sliding mode control (15).

$$S\dot{X} + \dot{\phi} = SA(x,t) + SB(x,t)d_{eq} + \dot{\phi} = 0 \quad (15)$$

Where  $d_{eq}$  is duty cycle input. The expression of equivalent control (16) is

$$d_{eq} = -(SB)^{-1}SA(x,t) \quad (16)$$

By substituting (5) into (15) the state space Eq. (17) derived is

$$\dot{X} = [I - B(SB)^{-1}S]A(x,t) \quad (17)$$

The above Eq. (17) represents the system dynamics under SMC.

### 3.2. Equivalent Controller using SMC

An equivalent translation of SM control law is adopted for PWM based ASMVC. The equivalent control signal  $ueq$ , a smooth function of discrete input function  $u$  is formulated using the invariance condition. The final duty ratio of pulse width modulator is derived from equivalent control function. The switching frequency is made constant using the new calculated duty cycle. Here, a reference term is added to the traditional sliding manifold (10) to form a new sliding

surface proposed is where, modified  $\phi = \int_0^t (v_o - v_r) dt$  and  $S = [\alpha, \beta]$

For buck converter:

The new existence condition of the changed sliding surface for the simplified model is given in (18)

$$\sigma(x,t)_{u=1} = \alpha \left( \frac{r_{loss} + Z_L}{Z_L} V_r + V_{in} \right) > 0 \quad (18)$$

The modified existing condition (19) is

$$\frac{Z_L V_{in}}{r_{loss} + R_L} - V_r > 0$$

$$-V_r < 0 \quad (19)$$

The reaching and existence conditions of both converters are the same for the original and simplified models. The unified sliding equivalent control becomes as shown in (20).

$$\overline{u_{eq}} = -[SB]^{-1}[SA(x,t) + (V_o - V_r)] \quad (20)$$

Now the choice of switching frequency is according to the open loop model of the converters. The proposed unified sliding mode equivalent controller expression (21) for buck converter is

$$\overline{u_{eq}} = \frac{\frac{\alpha}{L}(r_{loss}x_1 + x_2) - \frac{\beta}{C}\left(x_1 - \frac{x_2}{Z_L}\right) + (V_r - x_2)}{\frac{(\alpha V_{in})}{L}} \quad (21)$$

From the equivalent controller expressions (21) it is inferred that the numerator terms are the same as that of PID controller. The simplified controller expression is shown in (22)

$$\overline{u_{eq}} = \frac{\frac{\alpha}{L}(r_{loss}x_1 + x_2) - \frac{\beta}{C}i_c + (V_r - x_2)}{\frac{(\alpha V_{in})}{L}} \quad (22)$$

The controller expression (21) is called non-adaptive controllers. In addition to variation in input voltage, load impedance variations has to be considered to make the system adaptable and to get a better dynamic response. The closed loop system is obtained by substituting  $ueq$  in (7). The closed loop model is given in (23)

$$\dot{X} = \begin{bmatrix} -\frac{\beta}{\alpha C} & \frac{\beta - Z_L C}{\alpha Z_L C} \\ \frac{1}{C} & -\frac{1}{Z_L C} \end{bmatrix} X + \begin{bmatrix} \frac{1}{\alpha} \\ 0 \end{bmatrix} V_r \quad (23)$$

### 3.3. Modelling of ASM Controller

The equivalent SMC proposed operates under the assumption that the losses are known. So to estimate  $r_{loss}$  adaptive law (24) is designed by introducing a new state variable  $x_3$ .

$$\dot{x}_3 = \gamma V_r (V_r - x_2) \quad (24)$$

where  $\gamma$  is adaptive coefficient, which determines the



switching frequency of the controller. The selection of  $\gamma$  is made in order to achieve fast response. The optimal controller in [22] after introducing adaptive coefficient becomes as shown in [25].

$$\underline{u}_{eq} = \frac{\frac{\alpha}{L}(x_3 x_1 + x_2) - \frac{\beta}{C}i_c + (V_r - x_2)}{\frac{(\alpha V_{in})}{L}} \quad (25)$$

The closed loop state space averaged equation obtained is as follows [26].

$$\dot{X} = \begin{bmatrix} -\frac{\beta}{\alpha LC} & \frac{\beta - Z_L C}{\alpha Z_L C} & \frac{V_r}{Z_L} \\ \frac{1}{C} & -\frac{1}{Z_L C} & 0 \\ 0 & -\gamma V_r & 0 \end{bmatrix} X + \begin{bmatrix} \frac{1}{\alpha} \\ 0 \\ \gamma V_r \end{bmatrix} V_r \quad (26)$$

In this paper, discretization of ASMVC designed in the continuous-time domain is implemented. In simulations, systems are usually discretized using the Euler method, while a zero-order holder (ZOH) is used in practical implementation of the ASMVC. The resulting dynamics can be written as  $\dot{X} = Ax + Bu_{eq}$

The switching logic discussed in section 2.2. helps the state trajectory to follow the desired path. The next step in controller design is stability analysis.

### 3.4. Stability Analysis using Lyapunov stability criterion

To verify the proposed controller analytically global stability analysis is done using system equations derived in section 2. The Second Lyapunov Method was found on the so called energetic approach to stability analysis. In this method, the evolution of energy of a dynamic system over time for any positive definite function is studied. The dynamic system with decreasing energetic function along any trajectory has a stability property and the decreasing energetic function is called a Lyapunov function.

To prove stability of a system a continuously differentiable positive definite function  $V(x)$  is defined. The classical condition of Lyapunov function [27] can be written as

$$\dot{V}(x) = V^T(x) \dot{V}(x), f(t, \infty) < 0 \quad (27)$$

As  $dv/dx$  is always negative, the system is said to be asymptotically stable if apparently  $V$  decreases continuously, and the state must end up in the origin of the state space. To develop these concepts, from the sign of  $V$  and  $V'$ :

For negative  $dv/dx$  system is globally asymptotic, it is unstable if  $dv/dx$  is positive definite or semi definite and

if  $dv/dx$  is indefinite then it is not possible to decide about stability.

According to the statement of Lyapunov's criterion [28]

$$V = \frac{1}{2}S^2 > 0 \quad \text{and} \quad \dot{V} = S\dot{S} \quad (28)$$

if  $S \neq 0$ . Now, using above in buck converter system equations the stability criterion for SMC [29] is

$$V = \frac{1}{2}(V_o - V_r)^2 \quad (29)$$

The time derivative of Eq. (29) is given in (30)

$$\begin{aligned} \dot{V} &= (V_o - V_r) \frac{1}{C} V \left[ \frac{V_s}{V_o} i_{ref} - \frac{V_o}{Z_L} \right] \\ &= (V_o - V_r) \frac{1}{C} \left[ \frac{V_r^2}{V_o Z_L} - \frac{V_o}{Z_L} \right] \\ &= -(V_o - V_r) \frac{1}{CV_o} [V_o^2 - V_r^2] \\ &= -(V_o - V_r) \frac{1}{CV_o} (V_o - V_r)^2 (V_o + V_r) \end{aligned} \quad (30)$$

From the inequality (30) we can conclude that the time derivative of  $V$  is negative semi definite for  $V_{in} > 0$  and the system is globally stable.

To check for local stability, it is sufficient to prove that  $V$  is locally positive definite and derivative of  $V$  be locally negative definite. With this definition, the characterizations of stability and asymptotic stability, carry through to the local case. From [29] and [30], both local and global stability are inferred. The closed loop representation for buck converter is simulated and experimentally validated. The results are discussed in the following section.

## 4. Simulation results and discussions

The dynamic response of the ASM voltage controller for battery operated mobile phones is obtained by simulating a 150 mW buck converter for a load variation from 25mΩ to 100 mΩ. Is performed using MATAB/Simulink software.

### 4.1. Simulation results

Table 2 shows the specifications for buck converter. The effect of ASMVC on the output voltage and inductor current is observed for the following conditions in this section.

- Transient region (turn on region),
- Under line and load variations (disturbances)



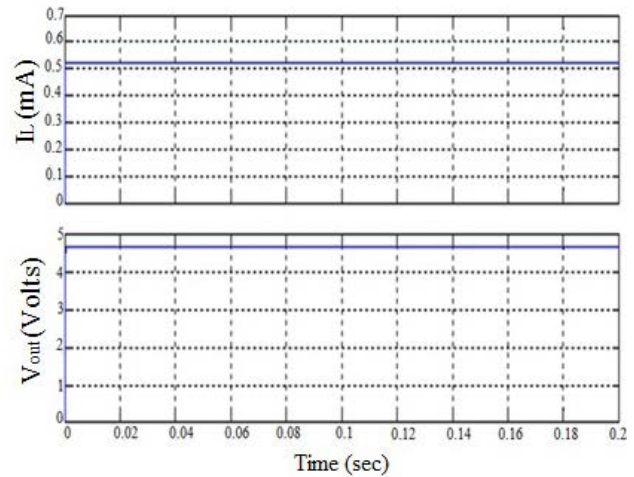
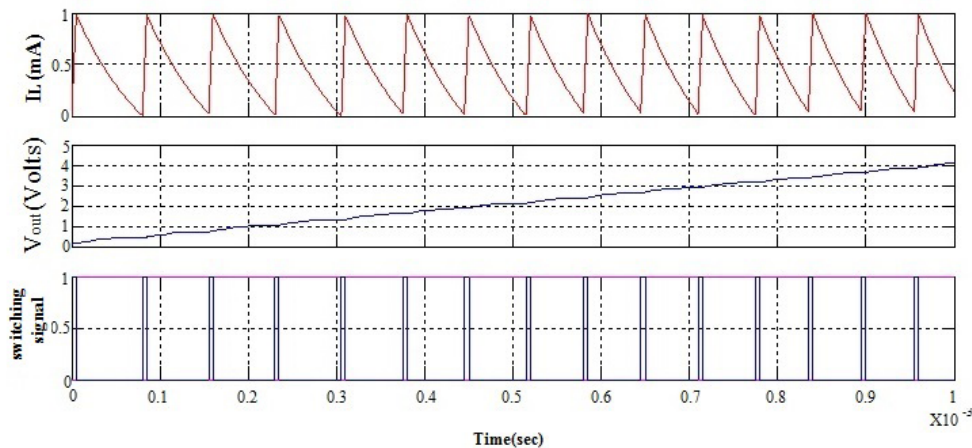
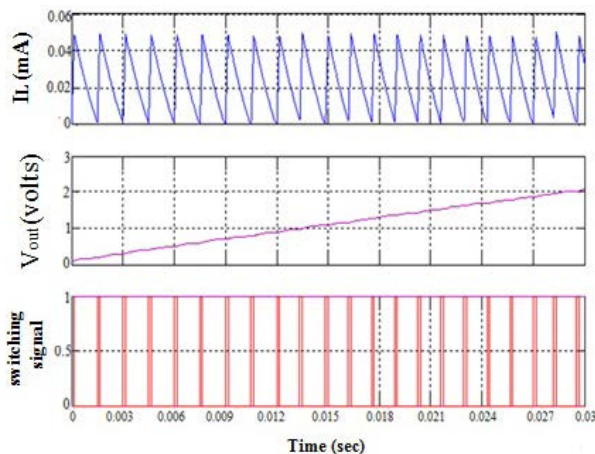
**Table 2 Buck Converter Specification**

Description	Parameter	Nominal Value
Input Voltage	$V_i$	6 V
Capcitance	C	47 $\mu$ F
Inductance	L	8.2 $\mu$ H
Switching frequency	$f_{sw}$	200KHz
Min. Load Impedance	$Z_{Lmin}$	25m $\Omega$
Max. Load Impedance	$Z_{Lmax}$	100m $\Omega$
Output Voltage	$V_o$	2 V

By examining Figure 4, it could be seen that the maximum overshoot of output voltage for SM controlled buck converter is 3.5 V, while the overshoot of inductor current is 100 mA. The maximum overshoot should not exceed 10% of the steady state value according to standards, but the maximum overshoot of the output voltage and inductor current is higher than 10%. The analysis of line and load variations reveals the following:

The effect of line variation was analyzed by applying a step change in the input voltage from 6 volts to 10 volts. It could be inferred from Figure 4 that SMC will force the

output voltage and inductor current to stay in a stable mode to infinitesimal change in the output voltage. The load was changed from 25m $\Omega$  to 100 m $\Omega$  and Figures 4, 5 and 6 shows the simulated waveforms for buck converter using SMC, ASMVC, and Digital ASMVC.

**Figure 4 Output voltage and Inductor current of SMVC Buck Converter****Figure 5 Output voltage and Inductor current of ASMVC Buck Converter****Figure 6 Output voltage and Inductor current of Digital ASMVC Buck Converter**

Load changes are made linearly from 25m $\Omega$  to 100 m $\Omega$ . As load value increases, the converter transfers its operation from CCM to DCM. The converter operates in CCM for changes from 15 m $\Omega$  to 45 m $\Omega$ . DCM starts at 50 m $\Omega$  during which output ripple voltage increases. The inductor current changes from CCM to DCM as load value changes from nominal load.

From the startup transient response of the buck converter using an SMC variation of the input voltage from 6 V to 10 V is analyzed. The settling time is 0.07 Sec at the nominal input voltage of 5V. The output profile is from 4 to 4.5 V. The settling time of the buck converter using SMC is 0.05 Sec for load changes from 25 m $\Omega$  to 100m $\Omega$  at nominal input voltage.

The buck converter output waveforms for same voltage changes using ASMVC are observed. The settling time was

**Table 3 Comparison of SM controller with ASM Controller**

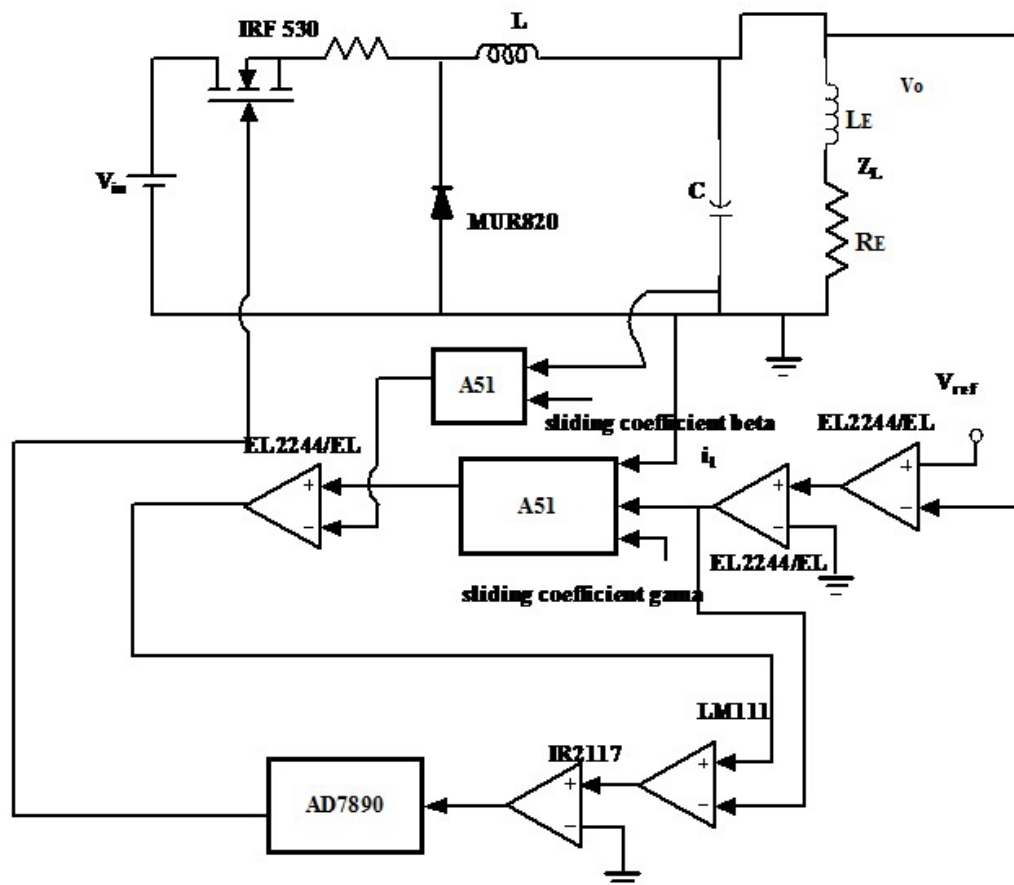
Type	Settling time ms	Rise time ms	Overshoot percentage %	Peak voltage V	Ripple voltage mV
SM controller	0.39	0.219	26.3	4.9	1.9
ASM controller	0.015	0.120	21	4.1	1.15
Digital ASM Controller	0.005	0.0212	5	2	0.245

about 0.0291 Sec at the nominal input voltage of 6 V. As the input voltage increases from 6 V to 10 V, the settling time decreases. The voltage profile changes from 3.5 to 4.1 V. For load changes from 25 mΩ to 100mΩ, The output voltage of the buck converter using ASMC settles at about 0.02 Sec.

A comparison between the PWM based sliding mode controller and ASM controllers for DC-DC buck converter is done. Unified Controller working at CCM and DCM for DC-DC converters are evaluated in simulation under the input voltage and load variation. The comparison between SM controller and ASM Controller is given in Table 3.

## 4.2. Prototype model of Converter

The circuit representation of the prototype model is shown in Figure 7. The operation is described as follows. The difference of output voltage and the reference voltage is fetched using EL2244/EL. The difference is integrated using opamp EL2244. After various synthesis stages the comparator LM111 output is fed to drive the circuit. The switching signal is converted to digital. Detecting CCM/DCM modification is achieved by comparator LM111. The output signal is fed to ADC 7890. Additionally, the output signal is applied to gate source of switching device IRF530.

**Figure 7 Prototype implementation of ASM controller**

The buck converter is experimentally validated by means of the hardware model shown in Figure 8.



**Figure 8** Experimental model of ASM controller

The simulated and experimental results for digital ASMVC buck converter for input voltage of 6 V with linear load impedance of 100mΩ is shown in Figures 6 and 9. An output voltage of 2 V is achieved in 0.03 ms. The simulation results for operation of buck converter during a voltage step from 6 to 10 V is shown in Figure 10.

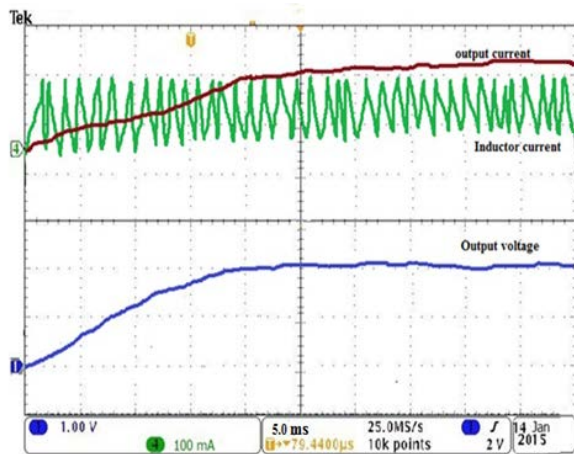


**Figure 9** Gate pulse and output voltage for Digitally controlled ASMVC converter with input voltage of 6 V

The reference voltage step is low-pass filtered by the EL2244 opamp resulting in a smooth voltage transient. The converter operates in DCM before the transient as seen from the discontinuous inductor current. It is shown that during the transient, the converter leaves DCM and enters CCM, whereas the output voltage remains unaffected from

this operation mode change and output voltage maintains at 2.4 V. After the transient, the buck converter operates in CCM. This experimental results shown in Figure 11 demonstrate that the proposed ASM controller enables a smooth transition between both operation modes of the converter and thus allows operating the buck converter within a wide load range.

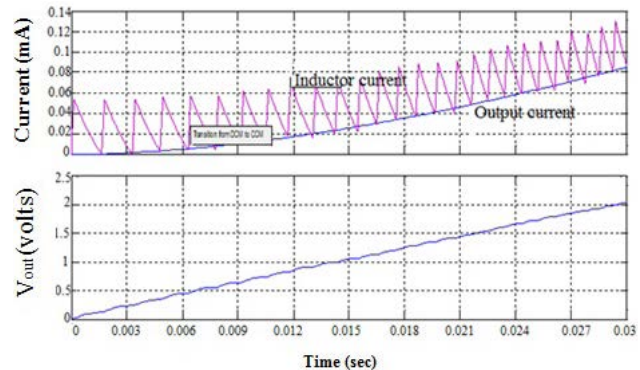


**Figure 10** Output and input voltage for step changes of 6 V to 10 V for Digital ASMVC buck converter

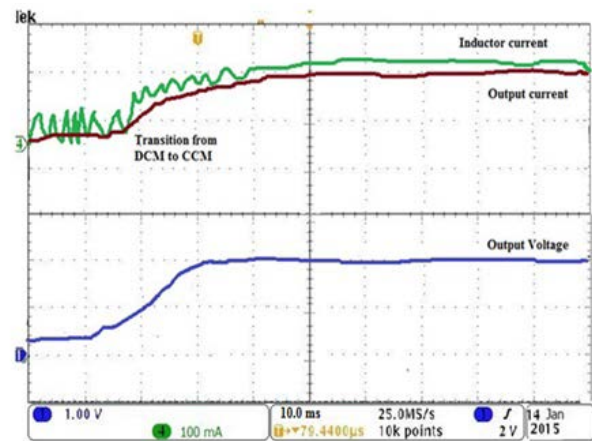


**Figure 11** Output and input voltage for step changes of 6 V to 10 V for Digital ASMVC buck converter

The prototype model responds the same as simulation model for line and load variations. Comparisons of simulated and experimental results are tabulated in Table 4 and represented graphically in Figures 12 and 13. The efficiency of the circuit is evaluated to check for power losses. The results show an efficiency of 95.5%. PWM based adaptive

**Table 4** Comparison of simulated model with experimental model for buck converter

Type	Settling time ms	Rise time ms	Overshoot percentage%	Peak voltage V	Ripple voltage mV
Simulated model	0.21	0.0212	1	2.1	0.245
Experimental model	0.31	0.02	1	2	0.299

sliding mode controller exhibits better performance under input voltages changes.

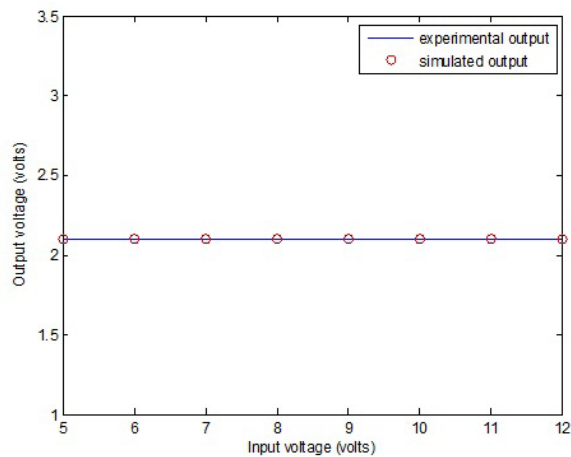


**Figure 12 Comparison of Simulated experimental output voltage**

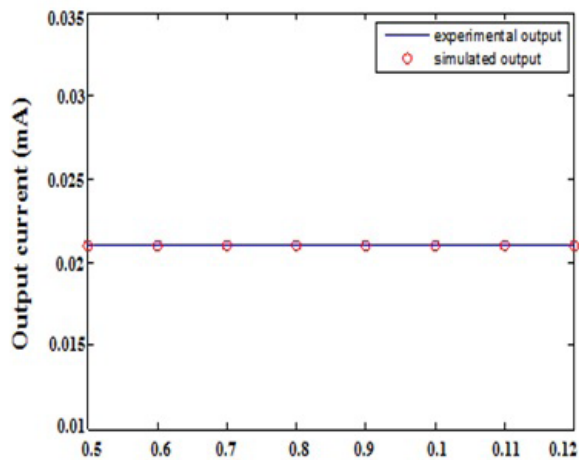


**Figure 13 Comparison of Simulated experimental output current**

## 5. Conclusion

A unified Digital ASM voltage controller for DC-DC buck converter working at CCM and DCM has been proposed and verified by computer simulation. The designed controller acts as input for mobile phones. The mathematical modeling and computer simulated verification of the PWM based ASMC have been presented. A gain scheduling scheme which monitors the output voltage and load current to vary the sliding line of the system is verified. The adaptive SM controlled converter has faster transient response with the reduced steady state error above the nominal load and ripple is minimized when operated below the nominal load. The output voltage and inductor current return to a steady state after line and load variation. Thus, the proposed converter system acquires the feature of achieving a stable steady-state response and swift transient response under varying operating points. In the future, the proposed unified controller shall be tested for all converters.

## 6. Acknowledgment

The authors are grateful to the management and principal of the ULTRA college of Engineering and Technology for Women and Velammal College of Engineering and Technology for providing all facilities for their research work.

## 7. References

1. M. Castilla, L. G. de Vicuña, J. M. Guerrero, J. Matas, and J. Miret, "Designing VRM hysteretic controllers for optimal transient response," *IEEE Transactions on Industrial Electronics*, vol. 54, no. 3, pp. 1726–1738, 2007.
2. S. R. Sanders, "Nonlinear control of switching power converters," Ph.D. dissertation, Massachusetts Institute of Technology, Cambridge, USA, 1989.
3. S. C. Tan, Y. M. Lai, C. K. Tse, L. M. Salameo, and C. K. Wu, "A Fast-Response Sliding-Mode Controller for Boost Type Converters with a Wide Range of Operating Conditions," *IEEE Transactions on Industrial Electronics*, vol. 54, no. 6, pp. 3276–3286, 2007.
4. J. Mahdavi, M. R. Nasiri, A. Agah, and A. Emadi, "Application of neural networks and state-space averaging to DC/DC PWM converters in sliding-mode operation," *IEEE/ASME Trans. Mechatronics*, vol. 10, no. 1, pp. 60–67, 2005.
5. D. Biel, E. Fossas, F. Guinjoan, E. Alarcon, and A. Poveda, "Application of sliding-mode control to the design of a buck-based sinusoidal generator," *IEEE Transactions on Industrial Electronics*, vol. 48, no. 3, pp. 563–571, 2001.
6. D. Ma and W. H. Ki, "Fast-transient PCCM switching converter with freewheel switching control," *IEEE Transactions on Circuits System II: Express Briefs*, vol. 54, no. 9, pp. 825–829, 2007.
7. S. C. Tan, Y. M. Lai, and C. K. Tse, "General Design Issues of Sliding Mode Controllers in DC-DC Converters," *IEEE Transactions on Industrial Electronics*, vol. 55, no. 3, pp. 1160–1173, 2008.
8. Z. Chen, "PI and sliding mode control of a Cuk converter," *IEEE Transactions on Power Electronics*, vol. 27, no. 8, pp. 3695–3703, 2012.
9. S. C. Tan, Y. M. Lai, and C. K. Tse, "A unified approach to the design of PWM-based sliding-mode voltage controllers for basic DC-DC converters in continuous conduction mode," *IEEE Transactions on Circuits and Systems I: Regular Papers*, vol. 53, no. 8, pp. 1816–1827, 2006.
10. G. Spiazzi and P. Mattavelli, "Sliding-mode control of switched-mode power supplies," in *The Power Electronics Handbook*, 3<sup>rd</sup> ed., T. L. Skvarenina (ed). Boca Raton, FL, USA: CRC Press, 2002.
11. H. Sira, "On the generalized PI sliding-mode control of dc-to-dc power converters: A tutorial," *International Journal of Control*, vol. 76, no. 9–10, pp. 1018–1033, 2003.
12. S. C. Tan, Y. M. Lai, M. Cheung, and C. K. Tse, "On the practical design of a sliding mode voltage controlled buck converter," *IEEE Transactions on Power Electronics*,



- vol. 20, no. 2, pp. 425–437, 2005.
13. E. Vidal, C. E. Carrejo, J. Calvente, and L. Martinez, "Two-Loop Digital Sliding Mode Control of DC–DC Power Converters Based on Predictive Interpolation," *IEEE Transactions on Industrial Electronics*, vol. 58, no. 6, pp. 2491–2501, 2011.
14. E. Fossas and A. Ras, "Second order sliding mode control of a buck converter," in *41<sup>st</sup> IEEE Conf. on Decision Control*, Las Vegas, NV, USA, 2002, pp. 346–347.
15. Y. B. Shtessel, A. S. Zinober, and I. A. Shkolnikov, "Boost and buck-boost power converters control via sliding modes using method of stable system centre," in *41<sup>st</sup> IEEE Conf. on Decision Control*, Las Vegas, NV, USA, 2002, pp. 340–345.
16. Y. B. Shtessel, A. S. Zinober, and I. A. Shkolnikov, "Boost and buck-boost power converters control via sliding modes using dynamic sliding manifold," in *41<sup>st</sup> IEEE Conf. on Decision Control*, Las Vegas, NV, USA, 2002, pp. 2456–2461.
17. S. C. Tan, Y. M. Lai, C. K. Tse, and M. K. Cheung, "Adaptive feedforward and feedback control schemes for sliding mode controlled power converters," *IEEE Transactions on Power Electronics*, vol. 21, no. 1, pp. 182–192, 2006.
18. C. Olalla, R. Leyva, I. Queinnec, and D. Maksimovic, "Robust gain-scheduled control of switched-mode DC–DC converters," *IEEE Transactions on Power Electronics*, vol. 27, no. 6, pp. 3006–3019, 2012.
19. V. Veselý and A. Ilka, "Gain-scheduled PID controller design," *Journal of Process Control*, vol. 23, no. 8, pp. 1141–1148, 2013.
20. P. Swarnkar, S. K. Jain and R. K. Nema, "Adaptive Control Schemes for Improving the Control System Dynamics: A Review," *IETE Technical Review*, vol. 31, no. 1, pp. 17–33, 2014.
21. M. Asif, M. J. Khan and N. Cai, "Adaptive sliding mode dynamic controller with integrator in the loop for nonholonomic wheeled mobile robot trajectory tracking," *International Journal of Control*, vol. 87, no. 5, pp. 964–975, 2014.